1   **Gut microbiota metabolically mediate intestinal helminth infection in Zebrafish**

2

3   Austin J. Hammer[1,*], Chris A. Gaulke[2,*], Manuel Garcia-Jaramillo[3], Connor Leong[1], Jeffrey

4   Morre[4], Michael J. Sieler[1], Jan F. Stevens[5,6], Yuan Jiang[7], Claudia S. Maier[4], Michael L. Kent[1],

5   Thomas J. Sharpton[1,7#]

6

7   [1]Department of Microbiology, Oregon State University

8   [2]Department of Pathobiology, University of Illinois Urbana Champaign

9   [3]Department of Environmental and Molecular Toxicology, Oregon State University

10   [4]Department of Chemistry, Oregon State University

11   [5]Department of Pharmaceutical Sciences, Oregon State University

12   [6]Linus Pauling Institute, Oregon State University

13   [7]Department of Statistics, Oregon State University

14

15

16

17   *Indicates the authors contributed equally to the manuscript

18

19

20   [#]**Corresponding Author**: Thomas J. Sharpton, E-mail: Thomas.Sharpton@oregonstate.edu

21   Department of Microbiology and Department of Statistics

22   Oregon State University, 97330

23
24
25
26
27
28

29   **Abstract**

30   Intestinal helminth parasite (IHP) infection induces alterations in the composition of

31   microbial communities across vertebrates, although how gut microbiota may facilitate or hinder

32   parasite infection remains poorly defined. In this work we utilized a zebrafish model to

33   investigate the relationship between gut microbiota, gut metabolites, and IHP infection. We

34   found that extreme disparity in zebrafish parasite infection burden is linked to the composition of

35   the gut microbiome, and that changes in the gut microbiome are associated with variation in a

36   class of endogenously-produced signaling compounds, N-acylethanolamines, that are known to

37   be involved in parasite infection. Using a statistical mediation analysis, we uncovered a set of

38   gut microbes whose relative abundance explains the association between gut metabolites and

39   infection outcomes. Experimental investigation of one of the compounds in this analysis reveals

40   salicylaldehyde, which is putatively produced by the gut microbe *Pelomonas*, as a potent

41   anthelmintic with activity against *Pseudocapillaria tomentosa* egg hatching, both *in vitro* and *in*

42   *vivo.* Collectively, our findings underscore the importance of the gut microbiome as a mediating

43   agent in parasitic infection and highlights specific gut metabolites as tools for the advancement

44   of novel therapeutic interventions against IHP infection.

45

46

47

48

49

50

51

52

53

54

Importance

Intestinal helminth parasites (IHPs) impact human health globally and interfere with animal health and agricultural productivity. While anthelmintics are critical to controlling parasite infections, their efficacy is increasingly compromised by drug resistance. Recent investigations suggest the gut microbiome might mediate helminth infection dynamics. So, identifying how gut microbes interact with parasites could yield new therapeutic targets for infection prevention and management. We conducted a study using a zebrafish model of parasitic infection to identify routes by which gut microbes might impact helminth infection outcomes. Our research linked the gut microbiome to both parasite infection, and to metabolites in the gut to understand how microbes could alter parasite infection. We identified a metabolite in the gut, salicylaldehyde, that is putatively produced by a gut microbe and that inhibits parasitic egg growth. Our results also point to a class of compounds, N-acyl-ethanolamines, which are affected by changes in the gut microbiome and are linked to parasite infection. Collectively, our results indicate the gut microbiome may be a source of novel anthelmintics which can be harnessed to control IHPs.

81 **Introduction**

82   Intestinal helminth parasitic infections present a significant global health burden,

83 affecting at least one quarter of the global population[1,2], and are disproportionately experienced

84 by individuals in impoverished nations, particularly children[3]. These infections are also

85 prominent among domestic animals[4,5], which places tremendous strain on livestock

86 management and veterinary practices[4,6,7]. Among infected individuals intestinal helminth

87 parasite (IHP) infections can contribute to anemia[8], cognitive impairment[9], physical wasting[10], as

88 well as a host of other conditions that contribute to the equivalent of millions of disability-

89 adjusted life years[11]. Unfortunately, the extreme burden of IHP infection may be exacerbated by

90 the emergence of drug-resistant parasites. High levels of broad anthelmintic drug resistance in

91 animal populations have been observed globally for decades[12,13] posing a tremendous risk to

92 humans because practices such as broad blanket anthelmintic administration[14] and prior

93 widespread prophylactic administration of anthelmintic drugs[15] have provided strong selective

94 forces for virulent drug resistant organisms[16]. While improved helminth management practice

95 may help slow the rate of anthelmintic resistance[16,17], the future of controlling IHP infection may

96 depend on innovating new methods and resources in anthelmintic discovery to stay ahead in

97 the pugilistic battle with drug-resistance in infectious nematodes.

98   In the search for new approaches to control intestinal helminth parasites (IHPs), there is

99 suggestive evidence that the intestinal microbiome can enhance or reduce parasite infection[18].

100 Microorganisms produce a diverse trove of metabolic compounds, including anthelmintic drugs.

101 For example, the avermectin class of compounds, which include the most widely administered

102 anthelmintic drugs on the planet, were originally derived from soil-borne bacteria such as

103 *Streptomyces avermectilis*[19]. Besides the soil, locations where helminths and microbes have

104 evolved to co-locate, such as the gut, may offer a rich resource of microbially derived

105 anthelmintic compounds[18] as their evolution by microbial community members may have been

106 critical to microbial exploitation of the shared ecological niche. However, the complex and

107   variegated metabolic landscape of microbially derived compounds which are found in the gut

108   and relevant to IHP infection remains unexplored.

109   Little is known about the existence of anthelmintic compounds derived from gut bacteria,

110   but it is known that gut microbiota can drive intestinal helminth infection through a variety of

111   mechanisms. For instance, bacteria can alter the protective integrity of mucosal barriers[20–23],

112   drive peristaltic activity[24,25], and produce inhibitory antibiotic compounds that limit pathogen and

113   parasite survival[19,26–28]. Moreover, signals from specific gut bacteria can cause egg hatching of

114   helminthic parasites in the gut, such as in the case of *Trichuris muris* infections in mice [29].

115   Additionally, gut microbes engage in extensive interaction with the vertebrate host immune

116   system[30], and intestinal helminths possess a diverse suite of immunomodulatory tools[31,32]. Much

117   of this cross-talk depends on the production of metabolite products by host, microbe, and

118   parasite. However, our current understanding of the complex set of metabolite interactions that

119   may directly or indirectly drive parasite colonization success is limited. Clarifying the set of

120   metabolites that mediate the interaction between host, parasites, and the gut microbiome may

121   provide a toolkit of compounds to control parasite infection.

122   Efforts to understand the role of the gut microbiome in health and disease conditions can

123   benefit from the application of analytic techniques that examine possible mediating roles of

124   intestinal microbes and metabolites. To this end, mediation inference techniques seek to

125   examine whether the relationship between two variables depends on the hypothesized

126   mediating effect of some third variable. While early iterations of these methods relied on

127   regression-based structural equation modeling[33] with strict assumptions regarding model type,

128   new methods are being innovated that account for data-specific assumptions, such as sparsity

129   and compositionality in microbiome data[34–37], and the suite of mediation tools available to

130   researchers is expanding rapidly. Recent applications of mediation analysis in microbiome

131   science have identified lipid compounds produced by *Akkermansia muciniphila* that modulate

132   murine immunity and metabolism[38], clarified the role of gut microbiota in mediating the

133   relationship between diet and immune inflammation[39], and established the role of the gut

134   microbiome in the development of childhood asthma[40]. However, the extension of mediation

135   techniques to high dimensional multi-omic data where there are a large number of both

136   independent and mediating features remains limited. Large sample sizes are often required to

137   attain sufficient power to detect mediating effects[41], which can impose substantial logistical

138   challenges on researchers seeking to use these techniques with expensive vertebrate models.

139   Despite this challenge, mediation techniques have played an important recent role in mapping

140   the gut microbiome to metabolites which may be involved in disease conditions such as

141   anorexia nervosa[42], and these methods offer a dynamic opportunity to ascertain the intricate

142   mechanisms by which the gut microbiome links to complex diseases, such as parasite infection.

143   Robustly identifying novel connections between the gut microbiome and parasite

144   infection via mediating metabolites presents a challenge that requires experimental investigation

145   using an organism that displays robust patterns of quantifiable IHP infection, displays a tractable

146   set of gut microbes, and may be scaled in the lab to deal with inherent statistical limitations of

147   mediation methods. In line with these requirements, the zebrafish model provides a powerful

148   tool for modeling parasite infections and shedding light on the intricate relationship between

149   host-microbiota interactions[43] and disease outcomes[44,45]. The model possesses a well

150   characterized taxonomic gut microbial composition[46,47] with a functional composition which

151   resembles that of humans[48], zebrafish offers a well-established model of intestinal helminth

152   parasite infection[49], and can be experimentally scaled in a cost-effective manner[50–52]. Zebrafish

153   have previously been used to discover and assay disease-related natural products[53–55] with

154   broad relevance. Collectively, the zebrafish-IHP model can be highly controlled to investigate

155   intricate routes by which the gut microbiome may mediate parasite infection, and insights

156   gleaned from connections between gut microbiota and gut metabolites may offer translational

157   potential for understanding the metabolite-based interactions between the gut microbiota,

158   intestinal helminth parasites, and the host.

159   In order to uncover gut microbial metabolites that mediate IHP infections, we used a

160   zebrafish model of intestinal helminth infection by the nematode *Pseudocapillaria*

161   *tomentosa*[49,56], as it affords access to the large sample sizes needed to disentangle these

162   relationships. In particular, instead of housing fish together we individually-housed parasite

163   infected fish hosts to understand why a small number of zebrafish bear a disproportionate

164   parasite burden in the absence of social or co-housing dynamics, and produced paired

165   microbiome and metabolome data from infected and uninfected fish to investigate links between

166   the microbiome, parasitic infection, and intestinal metabolites. We observed that the gut

167   microbiome explains the variation in infection burden across individuals. We then utilized a

168   mediation inference framework to identify microbe-metabolite interactions that statistically

169   mediate worm burden. This work reveals a potent anthelmintic, salicylaldehyde, whose effect on

170   infection burden is mediated by members of the gut microbiome. Analysis of the paired

171   microbiome-metabolome data also implicates N-acylethanolamines (NAEs) in the association

172   between microbiota and parasite infection burden. Collectively, our work demonstrates that the

173   zebrafish gut microbiome metabolically mediates IHP infection outcomes and reveals novel

174   microbiome-sourced anthelmintic drug leads.

175

176   **Results**

177   **Intestinal helminthic parasite infections are overdispersed among socially isolated**

178   **zebrafish**

179   IHP infections frequently manifest overdispersed distributions across wildlife populations,

180   agricultural settings, and scientific laboratories[57–59]. Prior work has shown that social behavior

181   and interactions can drive differences in parasite infection burden[60–62] but it remains unclear if

182   such behavior and interactions underlie the distribution of burden. For example, in zebrafish,

183   social hierarchies and behaviors[63–65] may impact feeding, which could result in interindividual

184   biases in oral exposure to infectious agents. To understand if zebrafish parasite burden

185   overdispersion occurs in the absence of co-housing or social dynamics, we individually housed

186   100 zebrafish in 1.2-L tanks and exposed 50 fish to *P. tomentosa* eggs. Stool samples were

187   collected from all surviving individuals at several time points: prior to *P. tomentosa* exposure,

188   immediately before exposure, and 29 days following parasite exposure, which prior work has

189   shown is the peak of infection[49,66]. At this final time, point fish were sacrificed and infection

190   burden was quantified through cytological analysis of dissected intestinal tissue.

191   Interrogation of the distribution of infection burden among *P. tomentosa*-exposed fish 29

192   days post exposure (dpe) reveals that infection is overdispersed across the population

193   (σ^2/μ=4.719, Supplementary Figure 1), indicating that relatively small numbers of exposed

194   individuals carry the bulk of mature worms in their guts. Our investigation of socially isolated

195   individuals reveals that community social dynamics alone are not the sole drivers of

196   overdispersed helminth parasite worm burden among zebrafish populations and indicates that

197   other factors underlie this phenomenon.

198

199   **Gut microbiome composition associates with parasite exposure and infection burden**

200   Gut microbiomes display highly personalized forms across individuals[67,68], and variation

201   in gut microbial communities has been consistently linked to parasite infection[66,69,70]. Thus, it is

202   conceivable that overdispersion in parasite infection burden outcomes results from the intricate

203   interplay between parasite exposure and gut microbiome composition that occurs in each

204   individual, where bacterial consortia could tip the scales toward susceptibility or resilience. We

205   investigated if zebrafish gut microbiome community structure is related to parasite exposure and

206   subsequent overdispersion of parasite infection burden. To investigate how gut microbiome

207   composition changes before and after parasite exposure, we generated 16S rRNA gene

208   sequence data from stool samples collected at both a pre-exposure baseline and at 29 days

209   post-exposure (dpe). In order to test whether the initial microbial community state influences the

210   microbiome's association with infection burden at the peak of infection, we initially altered fish

211   gut microbial communities by administering antibiotics three days prior to *P. tomentosa* parasite

212   exposure (Fig. 1). This strategy was employed to ensure variability in the gut microbiome

213   compositions across the individually housed fish, which was necessary for analyzing the

214   potential role of the gut microbiome in parasite infection. The resultant microbial diversity

215   enabled us to explore the association between distinct microbiome profiles and the differential

216   parasite burden outcomes. Microbial communities at 29 dpe were significantly stratified by both

217   parasite exposure (PERMANOVA, F=7.1618, p<0.0001) as well as parasite burden

218   (PERMANOVA, F=12.1514, p<0.0001). These results are consistent with our earlier findings[66],

219   but in this case individually housing fish eliminates possible impacts of co-housing that may

220   drive homogeneity of the gut microbiome among infected versus non-infected individuals. Thus,

221   this design and these results provide particularly compelling evidence that zebrafish gut

222   microbial communities are connected to *P. tomentosa* and later infection success, and may

223   contribute to the overdispersion of infection burden across individuals.

224

225   **Effect of IHP exposure on the gut microbiome composition depends on the pre-exposure**

226   **microbiome state**

227   Given that parasite colonization and the effects of parasite infection have been linked

228   with gut microbiome composition in this work and elsewhere[71], we reasoned that altering the

229   initial state of the microbiome may shape its relationship to subsequent IHP infection. Analysis

230   of 16S rRNA gene sequences generated from fish stool collected after this antibiotic exposure

231   but prior to *P. tomentosa* exposure reveals that antibiotic administration successfully altered the

232   composition of the zebrafish gut microbiome (PERMANOVA, F=27.565, p<0.0001). A

233   corresponding analysis at 29 dpe shows that the relationship between fecal microbial

234   community composition and IHP exposure depends on this prior antibiotic exposure

235   (PERMANOVA, F=3.16, p=0.009). Moreover, we find that parasite infection burden is strongly

236   linked to the composition of the microbiome (PERMANOVA, F=7.1618, p<0.0001, Fig. 2), but

237   that this relationship fundamentally depends on whether hosts were exposed to antibiotics first

238   (PERMANOVA, F=4.2087, p=0.002). This interaction is particularly noteworthy because at 29

239   dpe no strong relationship is observed between the composition of the gut microbiome and

240   antibiotic exposure alone (PERMANOVA, F=1.32, p=0.2277). These findings collectively

241   suggest that perturbations to the initial state of the microbiome, such as through antibiotic

242   exposure, have a cryptic effect on the successional interplay between IHP infection and the gut

243   microbiome, even when the statistical effects of antibiotic exposure are no longer prominently

244   observed.

245   This observation may be of special interest given that geographic locales which have

246   higher levels of IHP infection also tend to be locations where microbiomes may be disrupted by

247   the use of antibiotics to manage bacterial infections[72,73]. Given the varied influential roles of the

248   microbiome on parasite infection[26–29], disruption of the initial microbiome state by antibiotics may

249   interfere with the ability of the microbiome to protect the host from helminth infection. Elucidating

250   how antibiotic use alters the microbes involved in helminth resistance, as well as their specific

251   interactions with parasites, is crucial. This knowledge could guide the development of

252   microbiome-based therapies that supplement those protective elements and reduce the adverse

253   impacts of helminth infection.

254

Fecal metabolites, including salicylaldehyde and N-acylethanolamines, inversely

associate with helminth infection burden

257   Metabolic products convey information about the presence of pathogens and

258   microbes[70,74], produce signals that underlie immune control[75], and interact within a complex

259   network of gut microbes, the host immune system, and invading parasites, driving shifts in the

260   intestinal environment. In order to understand the metabolomic landscape wherein zebrafish gut

261   microbes and parasites co-locate, we performed untargeted metabolomic profiling of the fecal

262   samples collected from the same individuals and at the same time point as our microbiome

263   profiling analysis. Prior research has shown that the zebrafish gut metabolome is composed of a

264   diverse array of lipids and fatty acids[76,77], as well as amino acids and various biogenic

265   amines[78,79]. Consistent with previous research, our annotated gut metabolomic data is also

266   dominated by a large number of complex lipids, vitamin and amino acid derivatives, as well as

267   polar metabolites from many compound classes. We first sought to find metabolites from this

268   diverse metabolite set that are statistically associated with parasitic worm burden. Due to the

269   high level of overdispersion frequently observed in parasite infection data[57–59] we utilized

270   negative-binomial generalized linear models (GLMs) to examine the statistical relationship

271   between a set of 303 annotated metabolites and *P. tomentosa* worm burden. We uncovered 35

272   metabolites which associate with parasite worm burden among infected hosts (Negative

273   Binomial GLM, FDR<0.1, Supplementary Table 1).

274   Numerous compounds which are associated with helminth parasite worm burden have

275   also been linked to parasite infection in other work. Salicylaldehyde, a compound previously

276   noted as a soil and plant nematicide[80–82] shares an inverse relationship with worm burden. This

277   analysis also identifies compounds which have previously been linked to parasite infection such

278   as a major form of Vitamin E, gamma-tocopherol[83]. Additionally, at 29 dpe we find that 6 of the 8

279   compounds classed as N-acylethanolamines (NAEs) such as oleoyl ethanolamide (OEA),

280   linoleoyl ethanolamide (LEA), 2-linoleoyl glycerol, and related N-acylethanolamine (NAE)

281   precursor compounds (e.g., glycerophospho-N-oleoyl ethanolamine), manifest an abundance

282   profile that sharply distinguishes infected versus uninfected individuals, where infected

283   individuals display higher metabolite abundances (Wilcoxon-Rank Sum Test, p<0.05, Fig. 3a).

284   Furthermore, six of the eight NAE-related compounds in these data are strongly inversely

285   associated with parasite worm burden (Negative Binomial GLM, FDR<0.1, Fig. 3b,

286   Supplementary Table 1).

287   The NAE class of metabolites represents a broad family of lipid messengers that play a

288   well-established role in energy metabolism and feeding behavior[84–86], as well as inflammation[85],

289   and prior work has established a relationship between the gut microbiome and NAEs[87–89], so we

290   next tested if the abundance of these metabolites is related to microbiome composition and

291   antibiotic exposure. Strikingly, we observed a robust association between the abundance of

292   these NAE compounds and gut microbiome composition at a time point prior to parasite

293   exposure and following antibiotic treatment. (PERMANOVA, p<0.05, Supplementary Table 2).

294   Notably, at this time there is evidence that the relationship between the zebrafish gut

295   microbiome and the abundance of six NAEs depends on whether or not fish were exposed to

296   prior antibiotics (PERMANOVA, p<0.1, Supplementary Table 2). These results are further

297   underscored by our finding that the composition of the gut microbiome at 29dpe is still strongly

298   linked to NAE abundance for six different compounds (PERMANOVA, p<0.0002,

299   Supplementary Table 2). Furthermore, the relationship between the gut microbiome and NAEs

300   is underscored by our results that show antibiotic exposure interacts with NAE abundance in a

301   manner that is significantly related to gut microbiome composition for five of the eight NAE

302   metabolites (PERMANOVA, p<0.0002, Supplementary Table 2).

303   These findings reinforce the emerging view that the gut microbiome plays a fundamental

304   role in regulating NAE levels, an observation which is especially noteworthy because recent

305   work has shown that intestinal nematodes which infect humans, mice, and even insects have

306   genes that encode functions for degradation of NAEs[90]. The collective impact of our NAE

307   analysis shows that their abundance is starkly different in parasite-uninfected versus infected

308   hosts, that NAE abundance is linearly related to parasite infection burden, and that the gut

309   microbiome is a principal driver of NAE abundance in zebrafish hosts. Given the multifaceted

310   role of NAEs in host physiology, immune response, and intestinal microbiome control, plus the

311   ability of IHPs to degrade and produce these compounds, emphasizes the significance of these

312   compounds as a nexus in the battle between helminth parasites and vertebrates host.

313

Connections between fecal metabolite abundance and *P. tomentosa* worm burden are putatively mediated by fecal microbiota

The prior analysis linking metabolites to parasite worm burden highlighted several compounds which are also known to drive changes in intestinal microbiome composition. Given the complex interplay between gut microbes and metabolite production, these findings open a line of inquiry into microbiome-metabolite interactions. Zebrafish gut microbial taxa have been linked to parasite infection[66], and given the connection between some of the aforementioned metabolites, such as NAEs, we hypothesized that the relationship between members of the gut microbial community and parasite infection depends on metabolite-related cross talk. In order to explore the interconnected role of metabolites, microbiota, and parasite worm burden we selected parasite burden-linked metabolites and prevalent taxa, then statistically analyzed individual metabolite-microbe pairings to identify relationships which may be relevant to parasite burden. Our workflow applied partial correlation to a set of worm burden linked metabolites and prevalent ASVs in order to identify microbe-metabolite associations which were robust after accounting for the controlling influence of other microbial taxa. Additionally, we used mediation inference methods to quantify whether a metabolite's statistical relationship to worm burden may be hypothetically mediated by members of the microbiota. The results of this approach provided a set of potential interactions between 25 metabolites and 17 members of the microbiota (Adjusted Causal Mediating Effect FDR<0.3, Fig. 4), whose microbe-metabolite relationship is uniquely strong in the context of other ASVs, and whose interacting relationship may be relevant to parasite infection.

One particular edge in this possible interaction set includes salicylaldehyde and an amplicon sequence variant (ASV) from the *Pelomonas* genera. Salicylaldehyde, also known as 2-hydroxybenzaldehyde, is an organic compound that occurs naturally in some foods such as buckwheat[91] and it is known that some salicylaldehyde derivatives exhibit antibacterial activity[92]. As described earlier, salicylaldehyde manifests a robust inverse relationship among parasite

340   exposed fish 29 days following parasite exposure (Fig. 5a) and the microbe to which it is

341   correlated, ASV 4, is one member of a small set of microorganisms in this work that are

342   negatively related to total helminth worm burden (Negative Binomial GLM p=0.002, Fig. 5b). In

343   addition to this inverse relationship following parasite infection, we also find that it is a

344   particularly important feature for predicting later parasite infection burden. We constructed a

345   random forest regression model considering parasite worm burden as a function of all gut

346   microbial taxa present prior to parasite exposure, and found that *Pelomonas*, specifically ASV 4,

347   shows up as one of the most important taxa for predicting parasite worm burden among a

348   feature set that includes hundreds of different microbial taxa (Supplementary Figure 2). This

349   same ASV is also strongly correlated with salicylaldehyde abundance (Spearman's Correlation,

350   ρ=0.62, p=0.002, Fig. 5c) and is predicted to mediate the relationship between salicylaldehyde

351   and worm burden (Average Causal Mediation Effect (ACME) FDR<0.3). Little is known about

352   the function and metabolic capacity of *Pelomonas*, but given its relationship with salicylaldehyde

353   and its strong inverse relationship with helminth worm burden we surveyed available *Pelomonas*

354   genomes available in the NCBI genome repository to understand if the taxonomic group

355   possesses genetic pathways associated with salicylaldehyde metabolism. Several available

356   *Pelomonas* genomes possess salicylaldehyde dehydrogenase[93], an enzyme responsible for

357   metabolism of salicylaldehyde, typically as part of the naphthalene degradation pathway[94], and

358   it has been long demonstrated that some taxa from the *Pelomonas* genera are capable of

359   metabolizing diverse polycyclic aromatic hydrocarbons (PAHs) including naphthalene[95].

360   *Pelomonas* metabolic capacity to interact with salicylaldehyde could very well explain the

361   predicted mediating role of this taxon in the relationship between salicylaldehyde and worm

362   burden.

363   We also found that the relationship between γ-tocopherol, which is a major form of

364   vitamin E, and parasite worm burden is putatively mediated by ASVs from the *Mycobacterium*

365   and *Pseudomonas* genera and parasite worm burden. The abundance of these ASVs was

366   positively linked to worm burden in this work (Negative Binomial GLM, FDR<0.05), and in an

367   earlier investigation the genera-level abundance of both of these taxa displayed a positive

368   correlation with IHP burden in zebrafish[66]. γ-tocopherol has been shown to modulate the

369   composition of the gut microbiome[83,96] and mitigate colitis caused by LPS-induced inflammation

370   signaling in mice[97], and reduced abundance of this metabolite leaves mouse hosts more

371   susceptible to helminth infections[98,99]. If this compound displays similar colitis mitigating and gut

372   microbiome altering effects in zebrafish, reduced abundance of this metabolite, either by

373   parasite infection or through metabolism by parasite-promoting taxa, may help clarify the basis

374   through which these members of the microbiota associate with increased worm burden.

375

376   **Salicylaldehyde administration completely inhibits *P. tomentosa* egg larvation**

377   To determine the anthelmintic effect of salicylaldehyde, we utilized both *in vitro* and *in*

378   *vivo* drug exposure assays to determine how exposure to the drug impacts *P. tomentosa*. One

379   mechanism common to many anthelmintic compounds such as albendazole and ivermectin is

380   inhibition of worm egg larvation[100]. Therefore, we innovated an *in vitro* assay to evaluate how

381   salicylaldehyde exposure impacts *P. tomentosa* egg larvation. Specifically, exposed 131 *P.*

382   *tomentosa* eggs to salicylaldehyde at a dose of 2mg/L, 136 eggs at 15mg/L, and a group of 242

383   eggs that were reared without exposure to salicylaldehyde. For each group, we quantified

384   larvation rates after 5 days. In the salicylaldehyde-unexposed group, 174/242 (72%) of the eggs

385   successfully larvated. Conversely, 0 eggs from either salicylaldehyde treated groups larvated

386   (Fisher's Exact Test, p<2e-16, Fig. 5d). The complete inhibition of egg larvation demonstrates

387   notable inhibition of egg-hatching in *P. tomentosa*.

388   We followed up on this finding by determining if salicylaldehyde can disrupt active *P.*

389   *tomentosa* infection *in vivo*. To do so, we exposed 60 fish to *P. tomentosa* parasite eggs, then

390   split the fish equally into 30 fish which were exposed to salicylaldehyde at a concentration of

391   2mg/L, and 30 fish that were not exposed to salicylaldehyde, but to a DMSO control. Mortality in

392   salicylaldehyde exposed and unexposed host fish was 10 and 5 fish, respectively, which started

393   at 16dpe. All examined moribund or fresh dead fish showed infections. The experiment was

394   terminated at 24 dpe, and the intestines of all surviving fish showed 100% infection in both

395   groups. Results indicate a slight reduction in infection burden among salicylaldehyde exposed

396   fish, with an average of 15 worms/fish in salicylaldehyde treated fish versus an average of 19

397   worms/fish among untreated controls (Wilcoxon Rank-Sum Test, p=0.3; Fig. 5e). Although more

398   strikingly, we found that drug treatment interfered with worm development: 7/25 (28%) the fish

399   that were not exposed to salicylaldehyde contained gravid female worms with eggs in their guts,

400   whereas no female parasites or free eggs were recovered from the salicylaldehyde-exposed

401   treatment group (Fisher's Exact Test, p=0.01, Fig. 5e).

402   Overall, these assays indicate that salicylaldehyde represents an enticing anthelmintic

403   drug lead, although further work is required to clarify the mechanism by which it acts, as well as

404   to explore specificity of IHP types it is active against. Furthermore, elucidating the potential

405   salicylaldehyde-producing capability of *Pelomonas* or other microbes may offer a microbiome

406   oriented route for control of parasite infection.

407

408   **Discussion**

409   The rise of anthelmintic resistant IHPs presents an exigent challenge to identify new

410   drugs and techniques to control IHP infection. To do so we must expand our understanding of

411   the factors that underlie infection, as this knowledge can be leveraged to design new biocontrol

412   strategies. Based on the historical discovery of novel anthelmintic compounds among bacteria[19]

413   as well as accumulating evidence that the intestinal microbiome affects the colonization success

414   of IHPs[18,69], we reasoned that exploring the metabolic landscape of the gastrointestinal

415   microbiota in the context of infection could unlock new leads in the quest for novel anthelmintic

416   strategies. To explore this idea, we investigated the relationship between gut microbes,

417   metabolites, and IHP infection in a zebrafish model using a multi-omic approach to statistical

418   mediation. In so doing, we identified a variety of metabolites that associate with infection burden

419   in a manner that is dependent upon specific microbial taxa. These relationships are valuable to

420   resolve not only because the metabolites and taxa in question may be utilized to develop novel

421   infection control strategies (e.g., anthelmintic drugs or probiotics), but because they underscore

422   the putative mechanisms by which the microbiome influences IHP infection outcomes.

423   Experimental validation of one particular lead, salicylaldehyde, reveals that our approach

424   can uncover microbially mediated compounds that elicit anthelmintic effects. Salicylaldehyde is

425   a nematicide used in agricultural settings and in our data is among the metabolites that are most

426   strongly inversely associated with worm burden. We performed follow up *in vitro* and *in vivo*

427   tests to confirm that salicylaldehyde elicits effects against *P. tomentosa*. In particular, this

428   compound completely inhibits *in vitro P. tomentosa* egg development and maturation. Cessation

429   of egg production following anthelmintic treatment is a common phenomenon with

430   gastrointestinal nematodes in production animals. For example, moxidectin has been

431   demonstrated to inhibit egg production in female worms of *Cooperia* that survive treatment in

432   the early stages of resistance[101]. We observe a similar phenomenon here, where there is a

433   complete absence of parasite worm eggs recovered from hosts that are exposed to

434   salicylaldehyde. Previous work has also shown that salicylaldehyde prevented hatching of the

435   potato cyst nematode, *Globodera pallida*[81], but this compound is not currently used for the

436   control of helminth infections in animal populations, and our experiments are the first to

437   demonstrate that this compound is also capable of inhibiting egg maturation in a parasite which

438   infects vertebrate organisms. While the precise mechanism of this action is uncertain, *P.*

439   *tomentosa* eggs have relatively delicate shells and are quite susceptible to desiccation and

440   chemical agents[102]. Thus, it is possible that salicylaldehyde either damages the egg shell

441   directly, or possibly translocates to unlarvated worms where it may impair their larvation

442   physiology. Future work should seek to uncover the specific mechanisms of action and whether

443   salicylaldehyde can elicit broad effects across IHP species that infect other hosts. Regardless,

444   our study suggests that repurposing salicylaldehyde as an anthelmintic drug against vertebrate

445   IHPs may help control infection in the face of rising multi-drug resistant IHPs.

446   As zebrafish are not capable of producing salicylaldehyde, we used statistical mediation

447   to identify a microbe from the *Pelomonas* genus as a potential source of the compound. In

448   particular, our mediation analysis finds that the relative abundance of *Pelomonas* positively

449   correlates with the abundance of salicylaldehyde and significantly explains the variation in the

450   underlying relationship between the compound and infection burden. While a variety of

451   processes may underlie these associations, prior work supports the hypothesis that these

452   patterns result from *Pelomonas*-induced metabolism of salicylaldehyde. The *Pelomonas* genus

453   is known to possess enzymes that may aid in the metabolism of salicylaldehyde, such as

454   salicylaldehyde dehydrogenase[93], and is a member of a diverse set of *Betaproteobacteria* which

455   are known to generate and utilize this compound during the degradation of naphthalene[94]. While

456   degradation of naphthalene represents one parsimonious explanation for the origin of

457   salicylaldehyde, another important alternative hypothesis regarding the origin and synthesis of

458   salicylaldehyde begins with phenylalanine. The results of our analysis point to phenylalanine as

459   a metabolite which is inversely related to parasite worm burden and whose relationship with

460   parasite worm burden is potentially mediated by *Pelomonas* (Fig. 4). The conversion of

461   phenylalanine to trans-cinnamic acid is known to be performed by bacteria[103–105]. The following

462   in a phenylalanine to salicylaldehyde metabolism might first require conversion of trans-

463   cinnamic acid to o-coumaric acid. The terminal conversion of o-coumaric acid to salicylaldehyde

464   is known in tobacco plants[106], as well as in a species of fungus[107], although bacterial catalysis of

465   this terminal reaction is not characterized. While this might represent a parsimonious

466   explanation for the biosynthesis of salicylaldehyde, more work is warranted to establish the

467   distribution of microbial participation in these pathways, especially with respect to *Pelomonas*.

468   Collectively, future research should seek to establish the precise route by which *Pelomonas*

469   synthesizes salicylaldehyde to affect IHP infections and whether related mechanisms exist

470   among the microbiota of other vertebrate hosts.

471   Our multi-omic analysis reveals substantial alterations in NAEs and NAE precursors

472   between parasitic infected and uninfected hosts, with a potential route of control by the gut

473   microbiome. Given that NAEs play in a broad range of physiological functions such as immune

474   regulation as well as energy metabolism and feeding behavior[84–86,108,109], IHPs are capable of

475   modulating NAEs to enhance infection[90], and their alteration is associated with changes in the

476   gut microbiome[87], these compounds represent a potentially rich area to understand the

477   intersection of parasite infection with the gut microbiome and host immune regulation. Our

478   results demonstrate that alteration of the gut microbiome by antibiotic exposure appears to drive

479   changes in NAE abundance that are sustained in the profile of several NAE compounds several

480   weeks after initial antibiotic exposure. The abundance of these compounds is also linked to IHP

481   infection and is linearly related to IHP infection burden. The NAE axis represents one route by

482   which the intestinal microbiome drives aspects of host physiology. The functions which are

483   regulated by NAE signaling such as feeding behavior and inflammation response are likely

484   relevant in explaining some aspects of parasite infection, especially given that parasites also

485   possess enzymes involved in regulating NAEs and their associated physiological functions. The

486   synthesis of these findings is complex, but elucidating the principal effects of NAE changes on

487   host physiology and parasite infection, in addition to identifying taxa whose abundance is

488   related to NAE changes, may reveal how intestinal microbiota participate in mediating host

489   response to IHPs and could reveal drug or probiotic targets that aid in control of helminth

490   infection.

491   While we highlight several compounds, such as salicylaldehyde and NAEs, which help

492   explain the relationship between the gut microbiome and parasite infection, there exists a rich

493   unexplored repository of metabolites in this data that may display similar anthelmintic activity.

494   To better understand the metabolomic landscape relevant to IHP infection, we modeled the

495   relationship between parasite burden and metabolite abundance and elucidated a collection of

496   compounds that may be harnessed and further investigated in efforts to control parasitic

497   colonization and success. For instance, trunkamide A, a compound that is of known bacterial

498   origin[110], and which has been examined for its antibiotic and antitumor activity[111], shows up as

499   being inversely associated with parasite burden in our data. Given the established ability of this

500   compound to be produced by bacteria, understanding its distribution among aquatic and

501   gastrointestinally associated bacteria may offer an enticing route to the discovery of novel

502   probiotic microbes which could be supplemented and stimulated to produce trunkamide A under

503   specific parasite-related conditions. Additionally, several compounds which have been explored

504   for anthelmintic activity, including baliospermin[112], and genistin[113], also show up in our results as

505   being significantly linked to parasite burden. Some of these metabolites may be of bacterial

506   origin, or modified by members of the gut microbiota, such as genistin[114], in a manner that

507   enhances their anthelmintic activity. Applying mediation methods to understand the possible

508   relationships between these compounds and microbes involved in parasite infection may help to

509   establish microbe-dependent routes for the control of parasite infection. Collectively, these

510   findings represent an additional set of metabolomic compounds that may be explored by mining

511   the gut microbiome for potential solutions to the urgent challenge posed by increasing

512   anthelmintic drug resistance.

513   In summary, this work unravels interactions within the zebrafish gut ecosystem, yielding

514   a deeper understanding of the dynamic relationships among microbiota, metabolites, and

515   parasitic infections. These results extend the application of mediation inference methodologies

516   to reveal specific bacterial metabolites that may serve as key mediators of host-parasite

517   interactions, and identifies novel anthelmintic drug leads. Notably, salicylaldehyde emerges as a

518   compelling anthelmintic compound, and we demonstrate its ability to inhibit parasitic egg

519   maturation in zebrafish. This work also establishes the involvement of other metabolites, like N-

520   acylethanolamines, in host-parasite-microbiome dynamics emphasizing the need for further

521   research to elucidate their influence. Collectively, our findings support the hypothesis that gut

522   microbiota play a role in parasite infection, and understanding the chemical means by which

523   microbiota are involved in helminth colonization may yield tools for infection control.

524

525   **Methods**

526   **Zebrafish Husbandry, Parasite Exposure, and Parasite scoring**

527   All zebrafish research was conducted under the approval of IACUC protocol 2022-0280.

528   Tropical 170 day old 5D zebrafish were obtained from the Sinnhuber Aquatic Research

529   Laboratory (Corvallis, OR). The fish were housed in a flow-through vivarium on a 14hr:10hr

530   light:dark cycle, and fed Gemma Micro 300 once a day, except on the weekends. Water

531   temperature was recorded daily and ranged from 23-28 C. There was also weekly testing of

532   ammonia (0-0.25ppm), pH (7.6), hardness (0-25 ppm), and conductivity (90-110 uS/cm) to

533   ensure high water quality. Prior to initial antibiotic exposure or parasite exposure, fish were

534   allowed to equilibrate in their tanks for 2 weeks. Each of the 100 fish used in this protocol was

535   randomly assigned to one of four unique exposure groups, no parasite and no antibiotic

536   exposure, no parasite and antibiotic exposure, parasite exposure and no antibiotics, and both

537   parasite and antibiotic exposure. After this period of equilibration, 50 out of the 100 fish were

538   exposed to a combination of antibiotics, 10mg/L colistin and 10mg/L vancomycin. Of the 100

539   fish used in the experiment, 50 were exposed to *P. tomentosa* eggs at a dose of 88 eggs per

540   fish.

541

542

543

544   **Zebrafish Gut Metabolite Mass Spectrometry**

545   Fecal pellets collected from individual zebrafish were promptly lyophilized to minimize

546   leaching of metabolomic content into water and then split approximately equally for use in

547   metabolomic and 16S rRNA library preparation and sequencing analyses. Due to the small

548   sample size and high water content of the fecal pellets, precise weighing was not feasible.

549   Therefore, total ion abundance normalization was implemented to account for variation in

550   sample input. Ivermectin and two isotopically labeled amino acids were incorporated into the

551   extraction mix to monitor injection accuracy and platform performance throughout the extended

552   batch run time. Zebrafish fecal samples were prepared for untargeted metabolomic analysis

553   using a modified extraction protocol. An extraction solvent consisting of equal parts 100%

554   ethanol (Sigma 1.11727.1000) and methanol (Fisher A456-1) was prepared and chilled

555   overnight at -20°C. Three 1.4mm zirconium oxide beads (VWR 10144-554) were added to each

556   2ml screw-top bead beating tube (Fisher 02-682-558). An extraction mix was then created by

557   diluting isotope standards (Cambridge Isotope Laboratories MSK-A2.1.2; 1:20 dilution) and

558   100µM Ivermectin standard (Sigma PHR1380) 1:10 in the chilled ethanol/methanol solution.

559   Twenty-five microliters of this extraction mix were added to each tube containing a fecal sample.

560   The samples were then homogenized using a Precelly's 24 bead beater (program: 2 x 5400 rpm

561   for 45s, 5s wait interval), centrifuged at 16,000 x g for 10 minutes at 4°C, and the resulting

562   supernatant (15-25µL) was transferred to glass vials (Microsolv 9532S-3CP-RS). In cases of

563   large sample volumes, an additional centrifugation step was performed.

564   Extracts were submitted for analysis using untargeted LC-HRMS/MS-based

565   metabolomics. An AB Sciex TripleTOF 5600 mass spectrometer coupled to a Shimadzu Nexera

566   UHPLC system was used as described previously[115]. Metabolite extracts were separated using

567   an Inertsil Phenyl-3 column (2.1 x 140 mm, 100 Angstrom, 5 µm; GL Sciences, Torrance, CA,

568   USA). Column was held at 50°C. We used a 50-minute binary gradient system consisting of:

569   Solvent A, water (LC-MS grade) with 0.1% v/v formic acid and solvent B, methanol (LC-MS

570   grade) with 0.1% v/v formic acid. Metabolites were eluted using the following gradient program:

571   1 min, 5% B; 11 min, 30% B; 23 min, 100% B; 35 min, 100% B; 37 min, 5% B; 37 min, 5% B

572   and 50 min, 5%B . Flow rate was 0.5 mL/min. Injection volume was 10 µL. Positive IonSpray

573   voltage was set to 5200 V, negative IonSpray voltage was set to 4200 V.   Source temperature

574   was 350°C. The q-TOF mass spectrometer was operated in the data-dependent mode using the

575   following settings: period cycle time 950 ms; accumulation time 100 ms; m/z scan range 50–

576   1200Da; and collision energy 40 V. Mass calibration of the TOF analyzer was performed

577   automatically after every fifth LC run.

578   LC-HRMS/MS data processing was performed with Progenesis QI software V2.0

579   (NonLinear Dynamics, United Kingdom) and ABSciex Masterview (ABSciex, USA) entailing

580   peak picking, retention time correction, peak alignment, and metabolite

581   identifications/annotations. Metabolite annotations was facilitated by Progenesis QI and

582   Masterview using an in-house spectral library base on the IROA Mass Spectrometry Metabolite

583   Library of Standards (MSMLS) containing retention times, exact mass and MS/MS information

584   of >650 metabolite standards (IROA Technologies, Bolton, MA, USA). This workflow allows

585   obtaining high confidence annotations (L1). In addition, tentative metabolite annotations were

586   obtained by searching the METLIN MS/MS library in Progenesis QI.

587

588   **Microbial 16S rRNA Library Preparation and Sequencing**

589   Fecal samples were collected from individual adult fish at Days 0, 3, and 32. Fish

590   mortality and parasite exposure precluded the collection of fecal pellets from every fish at all

591   time points. For samples and time points at which fecal samples could be collected, DNA was

592   isolated using the Qiagen DNeasy PowerSoil kit, in accordance with the manufacturer's

593   directions. After a 10-minute incubation at 65°C, samples were subjected to bead beating, using

594   0.7mm garnet beads, for 20 minutes using the Vortex Genie 2 (Fisher, Hampton, NH, USA).

595   PCR was performed in triplicate using 1 microliter of purified DNA from the lysis solution to

596   amplify the V4 region of the 16S rRNA gene, using the 806r and 515f primer set[116]. Amplified

597   DNA collections were quantified using a Qubit HS Kit (Carlsbad, CA, USA). An equal quantity of

598   DNA was selected from each of the 252 samples, for a total DNA mass of 200ng, and the

599   pooled collection of DNA was cleaned using the QIAGEN QIAquick PCR purification kit then

600   diluted to a final concentration of 10nM. The final pooled DNA collection was sequenced by the

601   Center for Quantitative Life Sciences at Oregon State University, using an Illumina MiSeq

602   instrument with 250-bp paired-end reads.

603

604   **Zebrafish Gut Microbiome Community Diversity Analyses**

605   Read quality filtering was performed using DADA2[117] with R 4.1.2. Alpha and beta-

606   diversity analyses were performed using a relative abundance-normalized sequence count

607   table. Generalized linear mixed effects models were used to model species richness and

608   Shannon diversity as a function of longitudinal timepoint, fish id, antibiotic exposure, parasite

609   exposure, and an interaction of antibiotic and parasite exposure. Bray-curtis dissimilarity and

610   subsequent NMDS ordination was performed using vegan[118]. To clarify how antibiotic

611   administration, parasite exposure, and other host factors relate to gut community composition

612   we used permutational multivariate analysis of variance (PERMANOVA, adonis2, vegan) with

613   10,000 permutations.

614

615   **Mediation analysis of gut bacteria and metabolites**

616   Regression-based mediation analysis was used to investigate the hypothesis that the

617   relationship between fecal metabolites to nematode parasite burden is mediated by the

618   abundance of gut microbiota. Briefly, the standard approach for these techniques employs

619   regression modeling to analyze the association between two variables, then models the

620   possible effect of a mediating variable on the relationship between the variables in the initial

621   model. We constrained the initial feature space by selecting metabolites for which annotation

622   and research-characterized biological identity was available. Sparsity of gut bacterial data

623   challenges statistical investigation of correlation, so only taxa whose relative abundance was

624   greater than 0 in more than 30% of samples were used. Microbiome data was normalized using

625 relative abundance, and the log of metabolite MS abundance was log transformed adding 1 to

626 initial values which were equal to 0. Initial feature selection yielded 40 prominent bacterial taxa,

627 and 27 metabolite compounds which were significantly related to worm burden (NB-GLM, FDR

628 < 0.1). We utilized the nptest package[119] to test for partial correlation for pairwise relationships

629 between metabolites and bacterial taxa. We applied partial correlation for each microbe-

630 metabolite pairing, and used all remaining taxa as conditioning variables to isolate direct

631 microbe-metabolite links. Pairings with an FDR-adjusted relationship <0.3 were considered.

632 Concurrently, ASV mediation of metabolite-parasite burden was tested using the mediation

633 package[120] in R, where metabolites were coded to represent high and low metabolite

634 abundances, with ASVs as mediators. Average causal mediation effect (ACME), average direct

635 effect (ADE), and proportion of direct effect mediated were calculated for each model of

636 microbe-metabolite pairing. Family-wise error rates were controlled by applying Benjamini-

637 Hochberg FDR correction (FDR<0.3) to partial correlation and ACME p-values for tested

638 mediating relationships. Visualizations of putative mediating interactions were visualized using

639 ggplot2[121]. Code to recreate the mediation analysis and visualizations is available here

640 (https://github.com/CodingUrsus/Zebrafish_Microbiome_and_Parasites).

641

642 **Salicylaldehyde Toxicity Assay**

643 A toxicity assessment identified the highest SA dose which did not result in significant

644 mortality. Adult zebrafish were aqueously exposed to SA in two 48 hr periods spaced 5 days

645 apart. The fish were monitored for any adverse health effects including mortality, and fish were

646 evaluated to ensure they were alive and capable of active movement. Toxicity endpoints were

647 evaluated from the initial exposure to 7 days after the last exposure. The chemicals used in this

648 study were salicylaldehyde (SA, cas: 90-02-8) and dimethyl sulfoxide (DMSO, cas: 67-68-5).

649 Salicylaldehyde was obtained from Tokyo Chemical Industries (lot: J052M-EQ) and DMSO was

650   purchased from VWR (lot: 22H2456964). Dilutions were made with 100% DMSO and stored in

651   closed vials in a desiccator at room temperature.

652   Fish were aqueously exposed to 0,1, 2, 3, 5, and 10 mg/L of SA with 0.01% DMSO. The

653   0-2 mg/L groups had two replicate tanks containing 16 males and 16 females. Furthermore, the

654   3-10 mg/L groups had 1 replicate tank containing 6 males and 6 females. The 3-10 mg/L

655   exposure groups were intended as positive controls, to ensure that null effects were not a result

656   of no chemical exposure.

657   Exposure groups 0-2 mg/L SAL occurred in 9L tanks first filled with 3L of system water

658   followed by 1mL of a concentrated SA stock solution. Following the addition of SA, the

659   remaining 3L of fish water was added to the tank to mix the chemical. The 3-10 mg/L exposures

660   were conducted in 2.8L tanks and followed the same chemical additional pattern. However, only

661   a total of 2L of water was added to the tank. Solutions were refreshed every 24 hrs using the

662   same method previously described. Lastly, each exposure tank was aerated with an air stone

663   and the fish were not fed, to preserve water quality.

664

665   **Parasite Salicylaldehyde Exposure Assays**

666   ***a. in vivo* Salicylaldehyde Exposure**

667   Based on our previous transmission studies[49,102], we experimentally infected 100 5D line

668   fish by placing them in a large tank from which ~30 infected fish were removed the day before.

669   The recipient fish were exposed in the infection tank for 5 days. *P. tomentosa* infection was

670   promoted within the tank by reducing the waterflow, not removing the detritus, and keeping fish

671   carcasses in the tank. Over a 5-day period, 1L of water from another infected tank was added to

672   the exposure tank to further enhance infection. After 5 days of exposure, the remaining fish

673   (~75) were randomly divided into four 9L tanks, two control tanks and two salicylaldehyde

674   exposure tanks.

675   Fish were then exposed to salicylaldehyde in the same manner as the toxicity trials in

676   their aquaria with the water turned off at 14-15 and 21-22 days post initial exposure (dpe). Using

677   the results of the toxicity trial, fish were dosed with either 2mg/L SA with 0.01% DMSO or 0.01%

678   DMSO (controls). Fish were monitored daily, and fresh dead fish were examined for the

679   presence of the worm. At 24 dpe, the infection status of the fish was evaluated using wet

680   mounts. The fish were first euthanized using a hypodermic shock. Following euthanasia, the gut

681   was dissected out of the fish and placed on a glass slide with a 60 X 24 mm coverslip with about

682   200 μL of water. The gut was compressed with a cover slip and viewed on a compound

683   microscope at 50 and 100x magnification. While viewing the guts the number of immature

684   worms, mature female eggs were counted. Each slide was read by two different readers within

685   about 20 min., and the average worm counts were used for future analyses.

686   **b. Egg Larvation Assay**

687   We tested the ability of SA to inhibit egg larvation through two separate trials in line with

688   previously used protocols[102]. Briefly, *P. tomentosa* eggs were collected by placing fish in a 10L

689   static tank for 2 days. After two days, the water was filtered through a custom 3D printed filter

690   apparatus fitted with 105, 40, and 25 μm nylon screens. The material retained on the 25 μm

691   screen was collected in 15 mL conical tubes and centrifuged at ~3,000 x g for 5 minutes. The

692   supernatant was decanted until 1ml of water remained.

693   In a first trial, collected eggs were exposed to 0, 2 or 15 mg/L of salicylaldehyde with

694   0.01% DMSO in 15 mL conical tubes. Eggs were transferred into each exposure group by

695   pipetting 200 μL of the egg pellet formed as described above into each conical tube. The

696   solution was homogenized and transferred to a 30°C room for incubation. *P. tomentosa* egg

697   larvation was quantified after 5 days of SA exposure (~10 days old). A second trial was

698   conducted where eggs were placed in a container on a shaker to aid in distribution of DMSO

699   control and SA throughout the egg-hatching solution. Eggs were exposed to 0, or 2 mg/L of SA

700   with 0.01% DMSO in 15 mL conical tubes, with the shaker on speed setting 2.5 (Hoefer, San

701   Francisco CA) throughout the exposure. Larvation of eggs was quantified 3 days after SA

702   exposure (~6 days old). In both trials, after exposure eggs were collected by centrifuging the

703   tubes at 5,000 rpm for 5 minutes. The eggs were subsampled by taking 20μL of water from the

704   bottom of the tube and placing them on a glass slide and covered with a glass 24x24 mm

705   coverslip. The number of larvated and unlarvated/dead eggs were counted using a compound

706   microscope at 50, 100 or 400x magnification.

707

708   **Acknowledgements**

714

715   **Data Availability**

716   The nucleotide data underlying the findings of this study are available in the NCBI

717   Sequence Read Archive (SRA) under BioProject ID PRJNA1132310, and annotated

718   metabolomic data from positive and negative ion modes are available here

719   (https://github.com/CodingUrsus/Zebrafish_Microbiome_and_Parasites/).

720
721   **References**
722
723   1. Maizels, R. M., Smits, H. H. & McSorley, H. J. Modulation of Host Immunity by Helminths:

724   The Expanding Repertoire of Parasite Effector Molecules. *Immunity* **49**, 801–818 (2018).

725   2. Hall, A., Hewitt, G., Tuffrey, V. & De Silva, N. A review and meta-analysis of the impact of

726   intestinal worms on child growth and nutrition. *Matern. Child. Nutr.* **4**, 118–236 (2008).

727   3. Crompton, D. W. T. & Nesheim, M. C. Nutritional Impact of Intestinal Helminthiasis During

728   the Human Life Cycle. *Annu. Rev. Nutr.* **22**, 35–59 (2002).

729   4. Charlier, J., Voort, M. van der, Kenyon, F., Skuce, P. & Vercruysse, J. Chasing helminths

730   and their economic impact on farmed ruminants. *Trends Parasitol.* **30**, 361–367 (2014).

731   5. Agriculture | Free Full-Text | Global Change and Helminth Infections in Grazing Ruminants

732   in Europe: Impacts, Trends and Sustainable Solutions. https://www.mdpi.com/2077-

733   0472/3/3/484.

734   6. Charlier, J. *et al.* Initial assessment of the economic burden of major parasitic helminth

735   infections to the ruminant livestock industry in Europe. *Prev. Vet. Med.* **182**, 105103 (2020).

736   7. Charlier, J., Höglund, J., von Samson-Himmelstjerna, G., Dorny, P. & Vercruysse, J.

737   Gastrointestinal nematode infections in adult dairy cattle: Impact on production, diagnosis

738   and control. *Vet. Parasitol.* **164**, 70–79 (2009).

739   8. Roche, M. & Layrisse, M. The nature and causes of 'hookworm anemia'. *Am. J. Trop. Med.*

740   *Hyg.* **15**, 1029–1102 (1966).

741   9. EZEAMAMA, A. E. *et al.* HELMINTH INFECTION AND COGNITIVE IMPAIRMENT AMONG

742   FILIPINO CHILDREN. *Am. J. Trop. Med. Hyg.* **72**, 540–548 (2005).

743   10. Raj, E., Calvo-Urbano, B., Heffernan, C., Halder, J. & Webster, J. P. Systematic review to

744   evaluate a potential association between helminth infection and physical stunting in

745   children. *Parasit. Vectors* **15**, 135 (2022).

746   11. Hotez, P. J. *et al.* The Global Burden of Disease Study 2010: Interpretation and Implications

747   for the Neglected Tropical Diseases. *PLoS Negl. Trop. Dis.* **8**, e2865 (2014).

748   12. Echevarria, F., Borba, M. F. S., Pinheiro, A. C., Waller, P. J. & Hansen, J. W. The

749   prevalence of anthelmintic resistance in nematode parasites of sheep in Southern Latin

750   America: Brazil. *Vet. Parasitol.* **62**, 199–206 (1996).

751   13. Van Wyk, J. A., Stenson, M. O., Van der Merwe, J. S., Vorster, R. J. & Viljoen, P. G.

752   Anthelmintic resistance in South Africa: surveys indicate an extremely serious situation in

753   sheep and goat farming. *Onderstepoort J. Vet. Res.* **66**, 273–284 (1999).

754   14. Gasbarre, L. C. Anthelmintic resistance in cattle nematodes in the US. *Vet. Parasitol.* **204**,

755   3–11 (2014).

756   15. Geerts, S. & Gryseels, B. Anthelmintic resistance in human helminths: a review. *Trop. Med.*

757   *Int. Health* **6**, 915–921 (2001).

758   16. Fissiha, W. & Kinde, M. Z. Anthelmintic Resistance and Its Mechanism: A Review. *Infect.*

759   *Drug Resist.* **14**, 5403–5410 (2021).

760   17. Nielsen, M. K., Kaplan, R. M., Abbas, G. & Jabbar, A. Biological implications of long-term

761   anthelmintic treatment: what else besides resistance are we selecting for? *Trends Parasitol.*

762   **39**, 945–953 (2023).

763   18. Sharpton, T. J., Combrink, L., Arnold, H. K., Gaulke, C. A. & Kent, M. Harnessing the gut

764   microbiome in the fight against anthelminthic drug resistance. *Curr. Opin. Microbiol.* **53**, 26–

765   34 (2020).

766   19. Burg, R. W. *et al.* Avermectins, New Family of Potent Anthelmintic Agents: Producing

767   Organism and Fermentation. *Antimicrob. Agents Chemother.* **15**, 361–367 (1979).

768   20. Johansson, M. E. V. *et al.* Normalization of Host Intestinal Mucus Layers Requires Long-

769   Term Microbial Colonization. *Cell Host Microbe* **18**, 582–592 (2015).

770   21. Petersson, J. *et al.* Importance and regulation of the colonic mucus barrier in a mouse

771   model of colitis. *Am. J. Physiol. Gastrointest. Liver Physiol.* **300**, G327-333 (2011).

772   22. Jakobsson, H. E. *et al.* The composition of the gut microbiota shapes the colon mucus

773   barrier. *EMBO Rep.* **16**, 164–177 (2015).

774   23. Liang, L. *et al.* Gut microbiota-derived butyrate regulates gut mucus barrier repair by

775   activating the macrophage/WNT/ERK signaling pathway. *Clin. Sci.* **136**, 291–307 (2022).

776   24. Waclawiková, B., Codutti, A., Alim, K. & El Aidy, S. Gut microbiota-motility interregulation:

777   insights from in vivo, ex vivo and in silico studies. *Gut Microbes* **14**, 1997296.

778   25. Obata, Y. *et al.* Neuronal programming by microbiota regulates intestinal physiology. *Nature*

779   **578**, 284–289 (2020).

780   26. Kommineni, S. *et al.* Bacteriocin production augments niche competition by enterococci in

781   the mammalian GI tract. *Nature* **526**, 719–722 (2015).

782   27. Zipperer, A. *et al.* Human commensals producing a novel antibiotic impair pathogen

783   colonization. *Nature* **535**, 511–516 (2016).

784   28. Sassone-Corsi, M. *et al.* Microcins mediate competition among Enterobacteriaceae in the

785   inflamed gut. *Nature* **540**, 280–283 (2016).

786   29. Hayes, K. S. *et al.* Exploitation of the Intestinal Microflora by the Parasitic Nematode

787   Trichuris muris. *Science* **328**, 1391–1394 (2010).

788   30. Zheng, D., Liwinski, T. & Elinav, E. Interaction between microbiota and immunity in health

789   and disease. *Cell Res.* **30**, 492–506 (2020).

790   31. Gazzinelli-Guimaraes, P. H. & Nutman, T. B. Helminth parasites and immune regulation.

791   *F1000Research* **7**, F1000 Faculty Rev-1685 (2018).

792   32. Maizels, R. M. & McSorley, H. J. Regulation of the host immune system by helminth

793   parasites. *J. Allergy Clin. Immunol.* **138**, 666–675 (2016).

794   33. Baron, R. M. & Kenny, D. A. The moderator-mediator variable distinction in social

795   psychological research: conceptual, strategic, and statistical considerations. *J. Pers. Soc.*

796   *Psychol.* **51**, 1173–1182 (1986).

797   34. Sohn, M. B. & Li, H. Compositional Mediation Analysis for Microbiome Studies. *Ann. Appl.*

798   *Stat.* **13**, 661–681 (2019).

799   35. Carter, K. M., Lu, M., Jiang, H. & An, L. An Information-Based Approach for Mediation

800   Analysis on High-Dimensional Metagenomic Data. *Front. Genet.* **11**, 148 (2020).

801   36. Zhang, H., Chen, J., Li, Z. & Liu, L. Testing for Mediation Effect with Application to Human

802   Microbiome Data. *Stat. Biosci.* **13**, 313–328 (2021).

803   37. Zhang, J., Wei, Z. & Chen, J. A distance-based approach for testing the mediation effect of

804   the human microbiome. *Bioinformatics* **34**, 1875–1883 (2018).

805   38. Zhang, Q. *et al.* Genetic mapping of microbial and host traits reveals production of

806   immunomodulatory lipids by Akkermansia muciniphila in the murine gut. *Nat. Microbiol.* **8**,

807   424–440 (2023).

808 39. Shi, H. *et al.* The gut microbiome as mediator between diet and its impact on immune

809   function. *Sci. Rep.* **12**, 5149 (2022).

810 40. Maturation of the gut microbiome during the first year of life contributes to the protective

811   farm effect on childhood asthma | Nature Medicine. https://www.nature.com/articles/s41591-

812   020-1095-x.

813 41. Schoemann, A. M., Boulton, A. J. & Short, S. D. Determining Power and Sample Size for

814   Simple and Complex Mediation Models. *Soc. Psychol. Personal. Sci.* **8**, 379–386 (2017).

815 42. The gut microbiota contributes to the pathogenesis of anorexia nervosa in humans and mice

816 | Nature Microbiology. https://www.nature.com/articles/s41564-023-01355-5.

817 43. Xia, H. *et al.* Zebrafish: an efficient vertebrate model for understanding role of gut

818   microbiota. *Mol. Med.* **28**, 161 (2022).

819 44. Phillips, J. B. & Westerfield, M. Zebrafish models in translational research: tipping the scales

820   toward advancements in human health. *Dis. Model. Mech.* **7**, 739–743 (2014).

821 45. Adhish, M. & Manjubala, I. Effectiveness of zebrafish models in understanding human

822   diseases—A review of models. *Heliyon* **9**, e14557 (2023).

823 46. Sharpton, T. J., Stagaman, K., Sieler, M. J., Arnold, H. K. & Davis, E. W. Phylogenetic

824   Integration Reveals the Zebrafish Core Microbiome and Its Sensitivity to Environmental

825   Exposures. *Toxics* **9**, 10 (2021).

826 47. Roeselers, G. *et al.* Evidence for a core gut microbiota in the zebrafish. *ISME J.* **5**, 1595–

827   1608 (2011).

828 48. Gaulke, C. *et al. An Integrated Gene Catalog of the Zebrafish Gut Microbiome Reveals*

829   *Significant Homology with Mammalian Microbiomes.* (2020).

830   doi:10.1101/2020.06.15.153924.

831 49. Kent, M. L., Gaulke, C. A., Watral, V. & Sharpton, T. J. Pseudocapillaria tomentosa in

832   laboratory zebrafish (Danio rerio): Patterns of infection and dose response. *Dis. Aquat.*

833   *Organ.* **131**, 121–131 (2018).

834 50. Nathan, J. & Kannan, R. R. Antiangiogenic molecules from marine actinomycetes and the

835   importance of using zebrafish model in cancer research. *Heliyon* **6**, e05662 (2020).

836 51. Yang, L. *et al.* Zebrafish embryos as models for embryotoxic and teratological effects of

837   chemicals. *Reprod. Toxicol.* **28**, 245–253 (2009).

838 52. Jia, H.-R., Zhu, Y.-X., Duan, Q.-Y., Chen, Z. & Wu, F.-G. Nanomaterials meet zebrafish:

839   Toxicity evaluation and drug delivery applications. *J. Controlled Release* **311–312**, 301–318

840   (2019).

841 53. Crawford, A. D. *et al.* Zebrafish Bioassay-Guided Natural Product Discovery: Isolation of

842   Angiogenesis Inhibitors from East African Medicinal Plants. *PLOS ONE* **6**, e14694 (2011).

843 54. Pitchai, A., Rajaretinam, R. K. & Freeman, J. L. Zebrafish as an Emerging Model for

844   Bioassay-Guided Natural Product Drug Discovery for Neurological Disorders. *Medicines* **6**,

845   61 (2019).

846 55. Delgadillo-Silva, L. F. *et al.* Modelling pancreatic β-cell inflammation in zebrafish identifies

847   the natural product wedelolactone for human islet protection. *Dis. Model. Mech.* **12**,

848   dmm036004 (2019).

849 56. Kent, M. L., Harper, C. & Wolf, J. C. Documented and Potential Research Impacts of

850   Subclinical Diseases in Zebrafish. *ILAR J. Natl. Res. Counc. Inst. Lab. Anim. Resour.* **53**,

851   126–134 (2012).

852 57. Crofton, H. D. A quantitative approach to parasitism. *Parasitology* **62**, 179–193 (1971).

853 58. Shaw, D. J. & Dobson, A. P. Patterns of macroparasite abundance and aggregation in

854   wildlife populations: a quantitative review. *Parasitology* **111 Suppl**, S111-127 (1995).

855 59. Rabajante, J. F. On Spatiotemporal Overdispersion and Macroparasite Accumulation in

856   Hosts Leading to Aggregation: A Quantitative Framework. *Diseases* **11**, 4 (2022).

857 60. MacIntosh, A. J. J. *et al.* Monkeys in the Middle: Parasite Transmission through the Social

858   Network of a Wild Primate. *PLOS ONE* **7**, e51144 (2012).

859 61. Ezenwa, V. O. & Worsley-Tonks, K. E. L. Social living simultaneously increases infection

860   risk and decreases the cost of infection. *Proc. R. Soc. B Biol. Sci.* **285**, 20182142 (2018).

861 62. Otterstatter, M. C. & Thomson, J. D. Contact networks and transmission of an intestinal

862   pathogen in bumble bee (Bombus impatiens) colonies. *Oecologia* **154**, 411–421 (2007).

863 63. Oliveira, R. F. Mind the fish: zebrafish as a model in cognitive social neuroscience. *Front.*

864   *Neural Circuits* **7**, 131 (2013).

865 64. Jones, L. J. & Norton, W. H. J. Using zebrafish to uncover the genetic and neural basis of

866   aggression, a frequent comorbid symptom of psychiatric disorders. *Behav. Brain Res.* **276**,

867   171–180 (2015).

868 65. Green, J. *et al.* Automated high-throughput neurophenotyping of zebrafish social behavior.

869   *J. Neurosci. Methods* **210**, 266–271 (2012).

870 66. Gaulke, C. A. *et al.* A longitudinal assessment of host-microbe-parasite interactions resolves

871   the zebrafish gut microbiome's link to Pseudocapillaria tomentosa infection and pathology.

872   *Microbiome* **7**, 10 (2019).

873 67. Turnbaugh, P. J. *et al.* A core gut microbiome in obese and lean twins. *Nature* **457**, 480–

874   484 (2009).

875 68. The Gut Microbiome and Individual-Specific Responses to Diet | mSystems.

876   https://journals.asm.org/doi/10.1128/msystems.00665-20.

877 69. Zaiss, M. M. & Harris, N. L. Interactions between the intestinal microbiome and helminth

878   parasites. *Parasite Immunol.* **38**, 5–11 (2016).

879 70. Leung, J. M., Graham, A. L. & Knowles, S. C. L. Parasite-Microbiota Interactions With the

880   Vertebrate Gut: Synthesis Through an Ecological Lens. *Front. Microbiol.* **9**, (2018).

881 71. Pickard, J. M., Zeng, M. Y., Caruso, R. & Núñez, G. Gut Microbiota: Role in Pathogen

882   Colonization, Immune Responses and Inflammatory Disease. *Immunol. Rev.* **279**, 70–89

883   (2017).

884   72. Browne, A. J. *et al.* Global antibiotic consumption and usage in humans, 2000–18: a spatial

885   modelling study. *Lancet Planet. Health* **5**, e893–e904 (2021).

886   73. Pullan, R. L. & Brooker, S. J. The global limits and population at risk of soil-transmitted

887   helminth infections in 2010. *Parasit. Vectors* **5**, 81 (2012).

888   74. Wang, L. *et al.* Microbiome-Metabolomics Analysis of the Impacts of Cryptosporidium muris

889   Infection in BALB/C Mice. *Microbiol. Spectr.* **11**, e02175-22.

890   75. Yang, W. & Cong, Y. Gut microbiota-derived metabolites in the regulation of host immune

891   responses and immune-related inflammatory diseases. *Cell. Mol. Immunol.* **18**, 866–877

892   (2021).

893   76. da Silva, K. M. *et al.* Mass Spectrometry-Based Zebrafish Toxicometabolomics: A Review of

894   Analytical and Data Quality Challenges. *Metabolites* **11**, 635 (2021).

895   77. Medriano, C. A. & Bae, S. Acute exposure to microplastics induces metabolic disturbances

896   and gut dysbiosis in adult zebrafish (*Danio rerio*). *Ecotoxicol. Environ. Saf.* **245**, 114125

897   (2022).

898   78. Aguilar, A. *et al.* Metabolomic Profiling Reveals Changes in Amino Acid and Energy

899   Metabolism Pathways in Liver, Intestine and Brain of Zebrafish Exposed to Different

900   Thermal Conditions. *Front. Mar. Sci.* **9**, (2022).

901   79. Sun, B. *et al.* Variability in fecal metabolome depending on age, PFBS pollutant, and fecal

902   transplantation in zebrafish: A non-invasive diagnosis of health. *J. Environ. Sci.* **127**, 530–

903   540 (2023).

904   80. Caboni, P. *et al.* Potent Nematicidal Activity of Phthalaldehyde, Salicylaldehyde, and

905   Cinnamic Aldehyde against Meloidogyne incognita. *J. Agric. Food Chem.* **61**, 1794–1803

906   (2013).

907   81. Danquah, W. B., Back, M. A., Grove, I. G. & Haydock, P. P. J. In vitro nematicidal activity of

908   a garlic extract and salicylaldehyde on the potato cyst nematode, Globodera pallida.

909   *Nematology* **13**, 869–885 (2011).

910   82. Bahiri, G. & Elliott, I. Composition containing salicylaldehyde nematicides and garlic extract.

911   (2013).

912   83. Choi, Y. *et al.* Vitamin E (α-tocopherol) consumption influences gut microbiota composition.

913   *Int. J. Food Sci. Nutr.* **71**, 221–225 (2020).

914   84. Hansen, H. S. & Diep, T. A. N-acylethanolamines, anandamide and food intake. *Biochem.*

915   *Pharmacol.* **78**, 553–560 (2009).

916   85. Tsuboi, K., Uyama, T., Okamoto, Y. & Ueda, N. Endocannabinoids and related N-

917   acylethanolamines: biological activities and metabolism. *Inflamm. Regen.* **38**, 28 (2018).

918   86. Mennella, I., Boudry, G. & Val-Laillet, D. Ethanolamine Produced from Oleoylethanolamide

919   Degradation Contributes to Acetylcholine/Dopamine Balance Modulating Eating Behavior. *J.*

920   *Nutr.* **149**, 362–365 (2019).

921   87. Fornelos, N. *et al.* Growth effects of N-acylethanolamines on gut bacteria reflect altered

922   bacterial abundances in Inflammatory Bowel Disease. *Nat. Microbiol.* **5**, 486–497 (2020).

923   88. Hasan, A. U., Rahman, A. & Kobori, H. Interactions between Host PPARs and Gut

924   Microbiota in Health and Disease. *Int. J. Mol. Sci.* **20**, 387 (2019).

925   89. Oleoylethanolamide treatment affects gut microbiota composition and the expression of

926   intestinal cytokines in Peyer's patches of mice | Scientific Reports.

927   https://www.nature.com/articles/s41598-018-32925-x.

928   90. Host- and Helminth-Derived Endocannabinoids That Have Effects on Host Immunity Are

929   Generated during Infection - PMC. https://www.ncbi.nlm.nih.gov/pmc/articles/PMC6204704/.

930   91. Janeš, D. & Kreft, S. Salicylaldehyde is a characteristic aroma component of buckwheat

931   groats. *Food Chem.* **109**, 293–298 (2008).

932   92. Antimicrobial Properties of Substituted Salicylaldehydes and Related Compounds.

933   https://www.degruyter.com/document/doi/10.1515/znc-2007-7-806/html.

934   93. salicylaldehyde pelomonas - Protein - NCBI.

935   https://www.ncbi.nlm.nih.gov/protein/?term=salicylaldehyde%20pelomonas.

936   94. Jia, B. *et al.* Evolutionary, computational, and biochemical studies of the salicylaldehyde

937   dehydrogenases in the naphthalene degradation pathway. *Sci. Rep.* **7**, 43489 (2017).

938   95. Stringfellow, W. T. & Aitken, M. D. Competitive metabolism of naphthalene,

939   methylnaphthalenes, and fluorene by phenanthrene-degrading pseudomonads. *Appl.*

940   *Environ. Microbiol.* **61**, 357–362 (1995).

941   96. Pham, V. T., Dold, S., Rehman, A., Bird, J. K. & Steinert, R. E. Vitamins, the gut microbiome

942   and gastrointestinal health in humans. *Nutr. Res.* **95**, 35–53 (2021).

943   97. Liu, K. Y., Nakatsu, C. H., Jones-Hall, Y., Kozik, A. & Jiang, Q. Vitamin E alpha- and

944   gamma-tocopherol mitigate colitis, protect intestinal barrier function and modulate the gut

945   microbiota in mice. *Free Radic. Biol. Med.* **163**, 180–189 (2021).

946   98. Smith, A. *et al.* Deficiencies in Selenium and/or Vitamin E Lower the Resistance of Mice to

947   Heligmosomoides polygyrus Infections. *J. Nutr.* **135**, 830–836 (2005).

948   99. Au Yeung, K. J. *et al.* Impact of vitamin E or selenium deficiency on nematode-induced

949   alterations in murine intestinal function. *Exp. Parasitol.* **109**, 201–208 (2005).

950   100.   Sutherland, I. A., Brown, A. E. & Leathwick, D. M. The effect of anthelmintic capsules on

951   the egg output and larval viability of drug-resistant parasites. *Vet. Res. Commun.* **27**, 149–

952   157 (2003).

953   101.   Yazwinski, T. A. *et al.* Control trial and fecal egg count reduction test determinations of

954   nematocidal efficacies of moxidectin and generic ivermectin in recently weaned, naturally

955   infected calves. *Vet. Parasitol.* **195**, 95–101 (2013).

956   102.   Kent, M. L., Watral, V., Villegas, E. N. & Gaulke, C. A. Viability of Pseudocapillaria

957   tomentosa Eggs Exposed to Heat, Ultraviolet Light, Chlorine, Iodine, and Desiccation.

958   *Zebrafish* **16**, 460–468 (2019).

959   103.   Xiang, L. & Moore, B. S. Biochemical Characterization of a Prokaryotic Phenylalanine

960   Ammonia Lyase. *J. Bacteriol.* **187**, 4286–4289 (2005).

961   104.   Moffitt, M. C. *et al.* Discovery of Two Cyanobacterial Phenylalanine Ammonia

962   Lyases: Kinetic and Structural Characterization,. *Biochemistry* **46**, 1004–1012 (2007).

963   105.   Lovelock, S. L. & Turner, N. J. Bacterial *Anabaena variabilis* phenylalanine ammonia

964   lyase: A biocatalyst with broad substrate specificity. *Bioorg. Med. Chem.* **22**, 5555–5557

965   (2014).

966   106.   Malinowski, J., Krzymowska, M., Godoń, K., Hennig, J. & Podstolski, A. A new catalytic

967   activity from tobacco converting 2-coumaric acid to salicylic aldehyde. *Physiol. Plant.* **129**,

968   461–471 (2007).

969   107.   Sarkate, A., Saini, S. S., Kumar, P., Sharma, A. K. & Sircar, D. Salicylaldehyde synthase

970   activity from *Venturia inaequalis* elicitor-treated cell culture of apple. *J. Plant Physiol.* **221**,

971   66–73 (2018).

972   108.   Kurlyandchik, I., Lauche, R., Tiralongo, E., Warne, L. N. & Schloss, J. Plasma and

973   interstitial levels of endocannabinoids and N-acylethanolamines in patients with chronic

974   widespread pain and fibromyalgia: a systematic review and meta-analysis. *Pain Rep.* **7**,

975   e1045 (2022).

976   109.   N-acylethanolamines, anandamide and food intake. *Biochem. Pharmacol.* **78**, 553–560

977   (2009).

978   110.   A global assembly line for cyanobactins | Nature Chemical Biology.

979   https://www.nature.com/articles/nchembio.84.

980   111.   Solution Structure of the Antitumor Candidate Trunkamide A by 2D NMR and Restrained

981   Simulated Annealing Methods | The Journal of Organic Chemistry.

982   https://pubs.acs.org/doi/full/10.1021/jo026464s?casa_token=KzS8l6i1jNwAAAAA%3AQRdq

983   pq0aHtclmJGnqlOBO1D3g2fnCeCGjq5fm9021ybsdCxDNJ8jK5QJpP-

984   bvMP93gFiXqJejPdu1b8.

985   112.   In vitro anthelmintic activity of Baliospermum montanum muell. arg roots - Document -

986   Gale Academic OneFile.

987   https://go.gale.com/ps/i.do?p=AONE&u=googlescholar&id=GALE|A178741632&v=2.1&it=r&

988   sid=AONE&asid=9e18e60e.

989 113.   Tandon, V. & Das, B. Genistein: is the multifarious botanical a natural anthelmintic too?

990   *J. Parasit. Dis. Off. Organ Indian Soc. Parasitol.* **42**, 151–161 (2018).

991 114.   Comparative metabolism of genistin by human and rat gut microflora: detection and

992   identification of the end-products of metabolism: Xenobiotica: Vol 32, No 1.

993   https://www.tandfonline.com/doi/abs/10.1080/00498250110085809.

994 115.   Kirkwood, J. S., Maier, C. & Stevens, J. F. Simultaneous, untargeted metabolic profiling

995   of polar and non-polar metabolites by LC-Q-TOF mass spectrometry. *Curr. Protoc. Toxicol.*

996   *Editor. Board Mahin Maines Ed.--Chief Al* **0 4**, Unit4.39 (2013).

997 116.   Apprill, A., McNally, S., Parsons, R. & Weber, L. Minor revision to V4 region SSU rRNA

998   806R gene primer greatly increases detection of SAR11 bacterioplankton. *Aquat. Microb.*

999   *Ecol.* **75**, 129–137 (2015).

1000 117.   Callahan, B. J. *et al.* DADA2: High resolution sample inference from Illumina amplicon

1001   data. *Nat. Methods* **13**, 581–583 (2016).

1002 118.   Dixon, P. VEGAN, a package of R functions for community ecology. *J. Veg. Sci.* **14**,

1003   927–930 (2003).

1004 119.   Helwig, N. E. Robust nonparametric tests of general linear model coefficients:

1005   A comparison of permutation methods and test statistics. *NeuroImage* **201**, 116030 (2019).

1006 120.   Tingley, D., Yamamoto, T., Hirose, K., Keele, L. & Imai, K. mediation: R Package for

1007   Causal Mediation Analysis. *J. Stat. Softw.* **59**, 1–38 (2014).

1008 121.   ggplot2 citation info. https://cran.r-project.org/web/packages/ggplot2/citation.html.

1009

1010

1011   Figure 1. Schematic of zebrafish husbandry and treatment events and timeline. 1) Briefly, 100 adult fish were placed in

1012   individual tanks, 2b) half of fish were subsequently exposed to antibiotics, 3b) then fish were randomly exposed to the

1013   zebrafish parasite Pseudocapillaria tomentosa. Fecal samples were collected 2a) prior to antibiotic exposure, 3a) just

1014   prior to parasite exposure, and 4) 29 days post-parasite exposure (dpe) after which fish intestinal histopathology was

1015   assessed. Samples were split and processed for untargeted fecal metabolomic analysis as well as fecal 16S rRNA

1016   DNA amplicon sequencing.

1017

1018   Figure 2. Principal Coordinates Analysis (PCoA) ordination of Bray-Curtis dissimilarity of microbiome communities at

1019   29 days following parasite exposure. Each point represents an individual fish. The halo intensity around points

1020   represents the number of quantified parasites in the gut at dissection. Point colors represent antibiotic exposed (blue)

1021   and unexposed (red) groups. The arrow illustrates an envfit relationship for worm burden, depicting the linear direction

1022   of association between parasite burden and Bray-Curtis dissimilarity.

1023

1024   Figure 3. (A) The abundance of N-Acyl-Ethanolamine related (NAE) compounds significantly differs between infected and uninfected

1025   fish. (B) NAE abundance inversely associates with parasite exposure for six of eight identified compounds. "*" indicates $p<0.05$, "**"

1026 $p<0.01$, and "***" $p<0.001$.

1027

1028

1029

1030   Figure 4. Network of microbe-metabolite interactions predicted to mediate parasite worm burden. Nodes represent fecal metabolites

1031   and gut bacteria. Edges represent statistically significant relationships, with colors indicating the direction of correlation (blue:

1032   positive, red: negative).

1033

1034   Figure 5. (A) Scatterplot of log salicylaldehyde abundance against worm burden among fish that are 29 dpe. (B) Scatterplot of

1035   *Pelomonas* ASV 4 relative abundance against worm burden among parasite exposed fish 29dpe. (C) Linear relationship between log

1036   salicylaldehyde abundance and *Pelomonas* relative abundance. (D) *P. tomentosa* eggs were exposed to salicylaldehyde at a

1037   concentration of 2mg/L in an *in vitro* assay. The y-axis depicts the % of eggs that are unlarvated or dead. (E) *in vivo* salicylaldehyde

1038   exposure assay comparing the number of mature female *P. tomentosa* worms that produced eggs.

1039

1040   Supplementary Figure 1. Distribution of mature *Pseucapillaria tomentosa* worms quantified during dissection of intestinal tissue 29

1041   days after initial helminth egg exposure.

1042

1043   Supplementary Figure 2. The ten most important features based on the increase in node purity for regression of helminth worm

1044   burden measured 29dpe on microbiota relative abundances at 0dpe, just prior to parasite egg exposure.
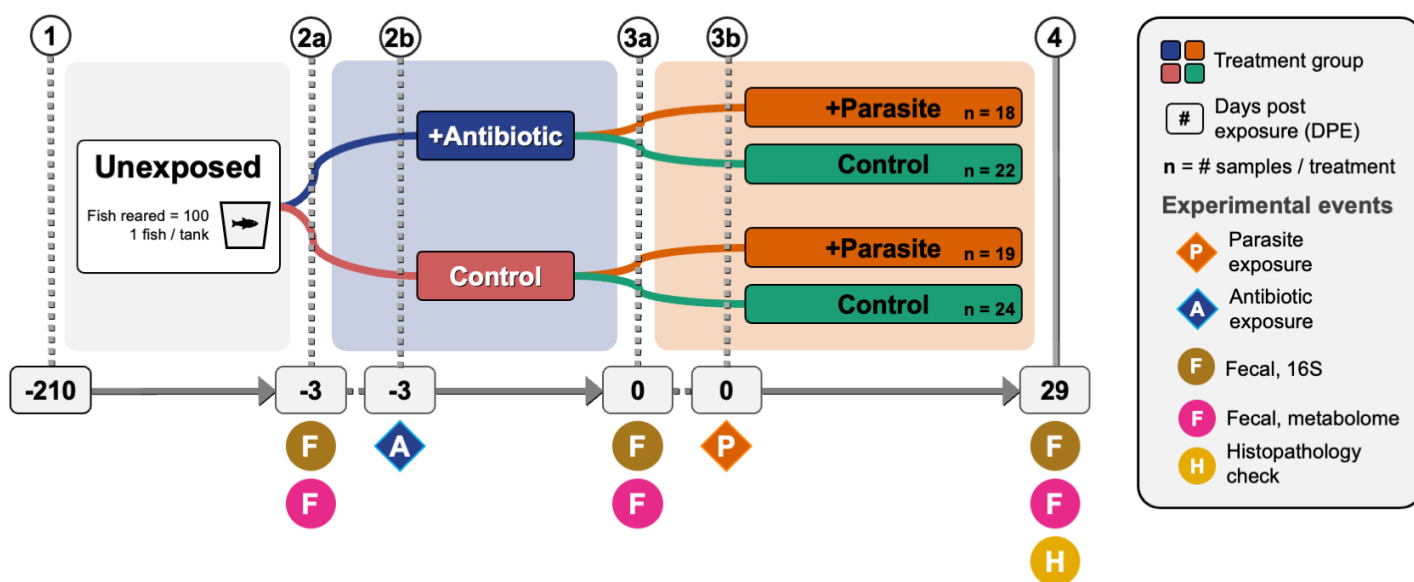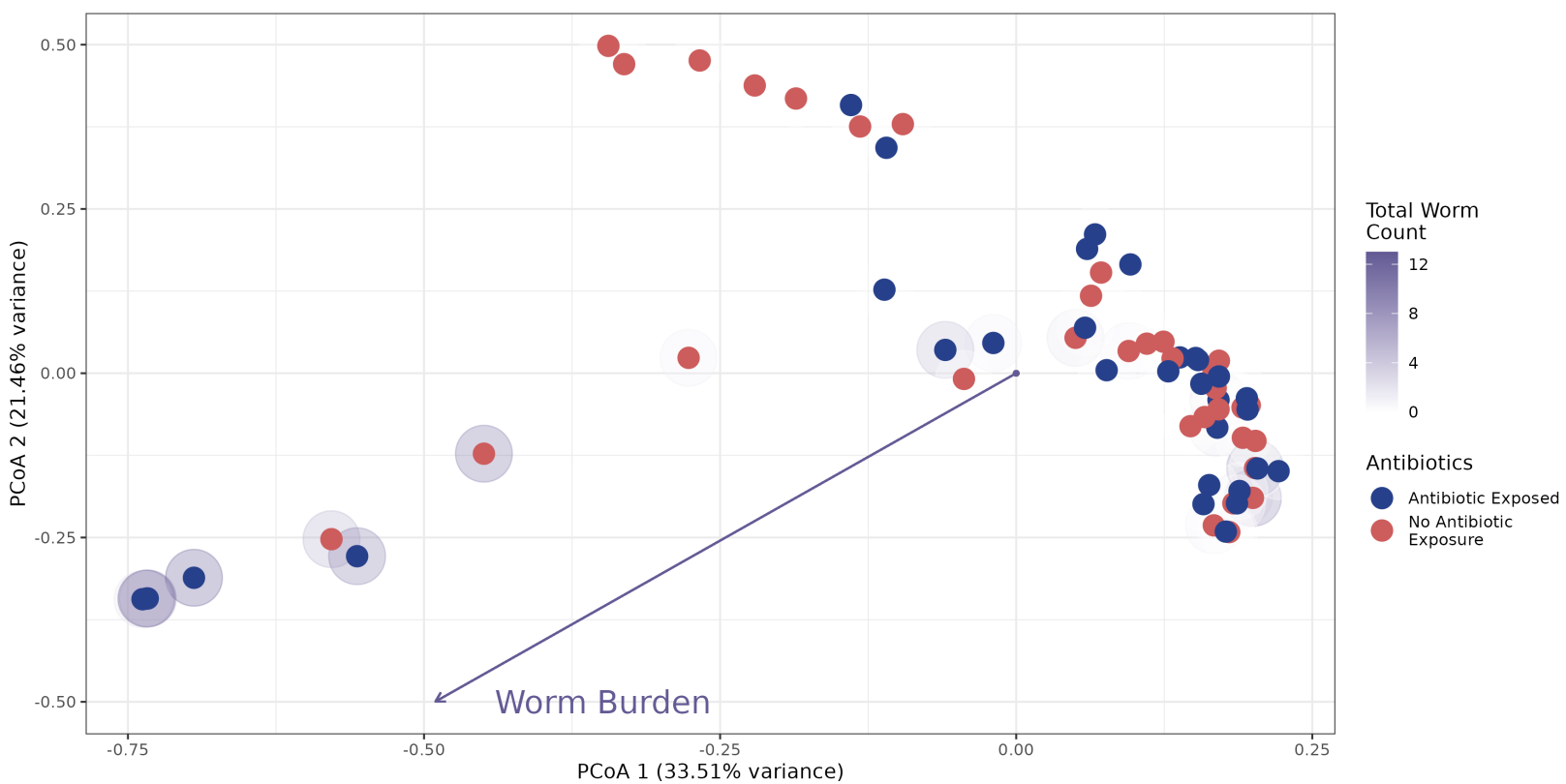
1045

1046   Supplementary Table 1. Coefficients table of metabolites which are linked to IHP burden (FDR<0.1) as measured 29dpe.
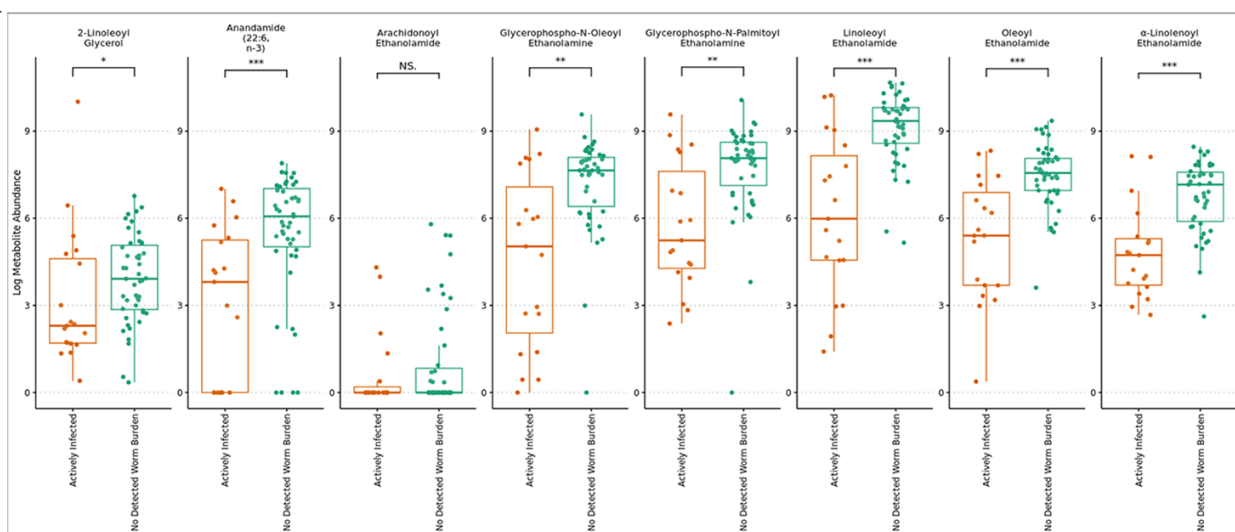
1047

1048   Supplementary Table 2. Coefficients table of PERMANOVA results testing the relationship between NAE abundance and microbiome

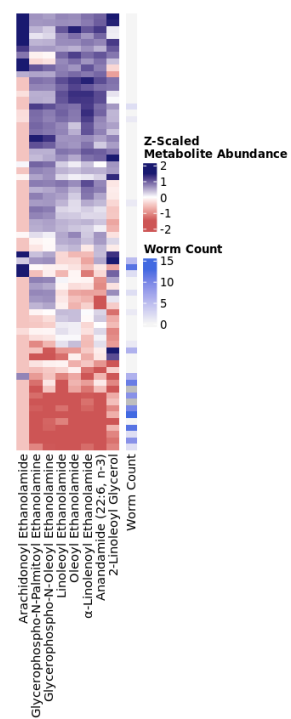1049   composition prior, as well as the interaction of NAE abundance and prior antibiotic exposure at 0dpe and 29dpe.